

# Mode-Locked Two-Photon States

Y. J. Lu, R. L. Campbell, and Z. Y. Ou  
 Department of Physics, Indiana University-Purdue University Indianapolis  
 402 N Blackford Street, Indianapolis, IN 46202  
 (March 29, 2024)

The concept of mode locking in laser is applied to a two-photon state with frequency entanglement. Cavity enhanced parametric down-conversion is found to produce exactly such a state. The mode-locked two-photon state exhibits a comb-like correlation function. An unbalanced Hong-Ou-Mandel type interferometer is used to measure the correlation function. A revival of the typical interference dip is observed. We will discuss schemes for engineering of quantum states in time domain.

Parametric down-conversion process is known to produce two-photon state with entanglement in a variety of degrees of freedom such as polarization [1], phases [2], frequency [3], and angular momentum [4]. Because of its relative ease of production, polarization entanglement is mostly used in applications in quantum information [5,6]. More recently, attention has been focussed on the spatial entanglement such as transverse modes [7]. With new degrees of entanglement discovered, there are more possibilities for information encoding. Among the entanglement properties, seldom discussed is the temporal entanglement. This is not a surprise if we consider the fact that the bandwidth ( $10^9$  Hz) of current optical detectors cannot match that of the down-conversion ( $10^{12}$  Hz). Nevertheless, frequency (complementary to time) entanglement was investigated recently for the potential nonlocal temporal shaping [8]. A similar investigation was done earlier by Zou et al [9]. Entanglement in the frequency domain involves infinite dimensions of continuous Hilbert space and therefore should exhibit far richer physical phenomena. In this letter, we will study directly the temporal entanglement in a special situation similar to a mode-locked laser and propose ways for quantum state engineering in the time domain by two-photon interference.

The concept of mode locking was first introduced to produce short pulses from a laser [10]. Normally a free running laser emits optical fields in continuous waves (CW) which consist of many independent longitudinal modes of different frequencies. When the modes of the laser are locked in phase, the output field becomes pulsed in a quasi-CW manner. The emitted pulses are spaced by the cavity round trip time. The temporal behavior of the field is simply a reflection of the Fourier transformation of the phase-locked frequency spectrum. Similarly, if the phases of different frequency components of a two-photon state are locked, the result is a mode-locked two-photon state of the form:

$$|j\rangle_{ML} = \sum_{m=0}^{N-1} d_m |j+m\rangle \otimes \sum_{p=0}^{N-1} \delta^{j+2m+2p} |j+2m+2p\rangle \quad (1)$$

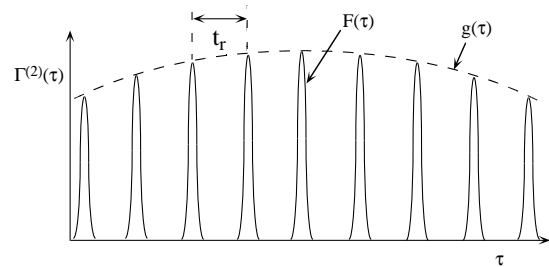


FIG. 1. Comb-like time correlation function of a mode-locked two-photon state in analogy to a mode-locked laser.

where  $N$  is the number of frequency modes of correlated photons,  $\Delta\omega$  is the frequency spacing between the adjacent modes, and  $g(\omega)$  gives the spectral distribution for a single mode. Different modes of photon pairs are in superposition, which provides the mechanism for phase locking. Photons in each pair are correlated in frequency. Such a state can be generated from a parametric down-conversion filtered by a Fabry-Pérot cavity. The different frequency components come from the longitudinal modes of the cavity.  $\Delta\omega$  is then the free spectral range of the cavity. All the pairs have a common origin (phase) from the pump field. The two-photon time correlation function can be calculated as

$$\begin{aligned} \Gamma^{(2)}(\tau) &= \langle \hat{E}^{(-)}(t) \hat{E}^{(-)}(t+\tau) \hat{E}^{(+)}(t) \hat{E}^{(+)}(t+\tau) \rangle \\ &= g(\tau) F(\tau)^2; \end{aligned} \quad (2)$$

where

$$g(\tau) = \int d\omega g(\omega) e^{i\omega\tau}; \quad F(\tau) = \frac{\sin[(2N+1)\Delta\omega\tau/2]}{\sin(\Delta\omega\tau/2)}$$

Since  $g(\omega)$  is the spectrum of single mode, it has much narrower bandwidth than the full bandwidth  $N\Delta\omega$ . So  $g(\tau)$  is a slowly varying function and  $\Gamma^{(2)}(\tau)$  is mainly determined by the function  $F(\tau)$ , which has a comb-like shape (Fig.1). The period of  $F(\tau)$  is the cavity round trip time  $t_r = 1/\Delta\omega$ . The physics behind Eq.(2) is the following: when a pair of photons enter the filter cavity, the cavity makes them bounce back and forth. Only

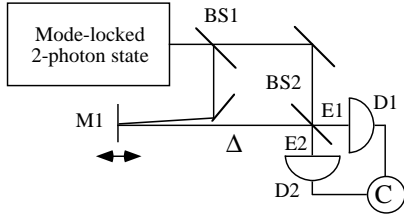


FIG. 2. Layout of the interferometer.  $\Delta$  is the time delay between the two arms.

when they hit the output coupler, is there some finite probability of escape and being detected. So the coincidence only occurs at a time interval that is a multiple of the round trip time of the cavity.

The comb-like time correlation function in Eq.(2) should be directly observable in a time delay distribution measurement, provided that the resolution time  $T_R$  of the detectors is smaller than the time interval  $t_c = 1/\Omega$ . Otherwise, the result is an average over the resolution time  $T_R$  in many periods of  $t_c$ :

$$\langle g^{(2)}(\tau) \rangle_{av} = A \langle |g(\tau)|^2 \rangle; \quad (3)$$

where  $A$  is a constant. So in the case of a poor detector resolution time, only the general contour of  $\langle g^{(2)}(\tau) \rangle$  can be observed and the comb-like feature is lost.

However, the comb-like feature in Eq.(2) can be indirectly observed by the method of two-photon interference with a variation of Hong-Ou-Mandel (HOM) interferometer [11] as shown in Fig.2. For a collinear type-I parametric down-conversion, the two correlated photons co-propagate and can be separated by a beam splitter (BS1). The second beam splitter (BS2) recombines the two photons to form the HOM interferometer. The whole setup is just a Mach-Zehnder interferometer. With two-photon detection at the outputs, it is also a Franson-type interferometer when the paths of the two arms are not balanced [12,13]. In a simple single mode model, the first beam splitter (BS1) transforms the input two-photon state into the following state:

$$|j_{BS1}\rangle = \frac{1}{\sqrt{2}}(|0i + j; 2i + \frac{P}{2}j; 1i\rangle); \quad (4)$$

The first two terms give the usual two-photon interference (interference between short-short and long-long paths) while the last term has no interference effect when the path difference is larger than the coherence length and normally provides a constant background if the detectors cannot resolve between the short and long paths. This will limit the maximum visibility to 50% [13]. With mode-locked two-photon input, however, the comb-like correlation function indicates that the  $|j; 1i$  state will reappear at a path delay of every multiple of  $t_c$ , the round trip distance of the filter cavity. When this happens, the last term will exhibit Hong-Ou-Mandel interference dip [11] at nonzero delays. The revival of HOM interference dips was first predicted by Shapiro [14].

The intuitive argument above can be easily confirmed by a calculation of the two-photon coincidence rate between the two detectors at the output of the unbalanced Mach-Zehnder interferometer in Fig.2. We use a multimode state given in Eq.(1) as the input state to the interferometer and obtain the result with 50:50 beam splitters as follows:

$$\begin{aligned} R_2(\tau) &= \langle \hat{E}_1^{(+)}(t) \hat{E}_2^{(+)}(t+\tau) \hat{E}_2^{(-)}(t+\tau) \hat{E}_1^{(-)}(t) \rangle \\ &= \frac{1}{2} g(\tau) F(\tau)^2 (1 - \cos \Omega \tau) + \\ &\quad + \frac{1}{4} g(\tau + \tau_c) F(\tau + \tau_c) g(\tau) F(\tau) \\ &\quad + \text{Re} [i \sin(\Omega \tau_c / 2) g(\tau) F(\tau) \{g(\tau + \tau_c) \\ &\quad F(\tau + \tau_c) - g(\tau) F(\tau)\}]; \end{aligned} \quad (5)$$

The last term gives no contribution when it is integrated over the detector's resolving time  $T_R$  that is larger than the time delay  $\tau$ . So the two-photon coincidence rate is proportional to

$$\begin{aligned} R_2(\tau) &= \int_{-T_R}^{T_R} d\tau' \langle g^{(2)}(\tau - \tau') \rangle \\ &= \frac{R_0}{2} (1 - \cos \Omega \tau) + \frac{R_0}{2} [1 - V(\tau)] \end{aligned} \quad (6)$$

where

$$\begin{aligned} R_0 &= \int_{-T_R}^{T_R} d\tau g(\tau) F(\tau)^2 \\ V(\tau) &= \frac{\int_{-T_R}^{T_R} d\tau' g(\tau' + \tau_c) F(\tau' + \tau_c) g(\tau') F(\tau')}{\int_{-T_R}^{T_R} d\tau' g(\tau') F(\tau')^2}; \end{aligned}$$

The first term in Eq.(6) corresponds to the first two terms in Eq.(4) and produces a phase sensitive two-photon interference pattern. The second term in Eq.(6) arises from the last term in Eq.(4) and gives rise to the HOM interference dip as  $\tau$  is scanned. Normally, there is only one dip around zero delay ( $\tau = 0$ ). But for mode-locked two-photon state, the reappearance of the coincidence peak at nonzero delays (due to the comb-like correlation function) will revive the HOM dips every time when the time delay  $\tau$  is such that  $F(\tau + \tau_c)$  overlaps with  $F(\tau)$ . This corresponds to  $\tau = M t_c = 2$  with  $M = \text{integer}$ . A surprising result is that the period of the revival of HOM dip is  $t_c = 2$  rather than  $t_c$  predicted from a previous simple intuitive argument and Ref. [14]. The shorter period can be understood if we take a detailed look at the timeline of photodetection in Fig.3 of an unbalanced HOM interferometer. The figure shows the interference of two possibilities: both photons are transmitted or both are reflected. In each case,  $2(l_1 - l_2)$  is the path difference between the two arms of the interferometer. Fig.3a corresponds to the intuitive argument: the two photons come from adjacent coincidence peaks with  $\tau = t_c$ . In Fig.3b, photodetections of the two photons are not simultaneous but have a time difference of  $t_c = 2$  [15]. The

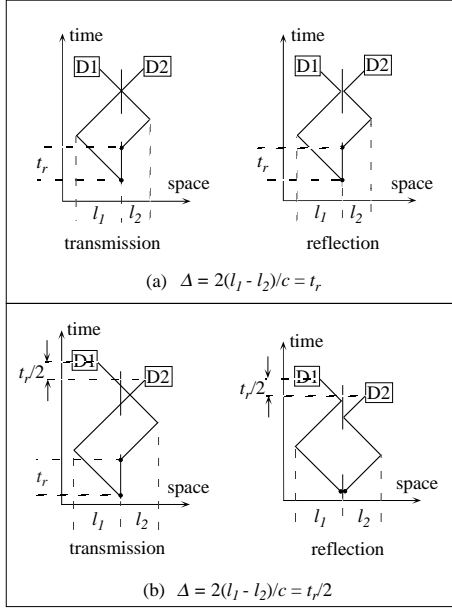


FIG. 3. Timeline for photodetection of two photons in an unbalanced HOM interferometer. See text for details.

two overlapping possibilities are from two different cases: two photons are separated by a delay of  $t_r$  or they are simultaneous. Because of mode lock nature of the process, the two possibilities are coherent to each other and will produce interference. In this case, we only need a time delay to be  $t_r = 2$ .

Although filtering after the generation of parametric down-converted photons will produce the required mode-locked two-photon state, it is at the expense of signal level, for the down-converted light signal is proportional to the detection bandwidth. Recently we have successfully implemented a type-I optical parametric oscillator (OPO) far below threshold for the generation of narrow band two-photon state without the reduction of the signal level [16]. Multimode operation of the device produces naturally a mode locked two-photon state. The cavity round trip time of the device is of the order of 1 ps, which prevents us from direct observation of the comb-like correlation function in Eq.(2). Nevertheless, we did observe the time average behavior predicted in Eq.(3) in a time delay distribution measurement.

To indirectly show the mode locking effect, we input the state into an unbalanced Mach-Zehnder interferometer as sketched in Fig.2 and observe the coincidence count between the two outputs as the mirror M1 is scanned. The mirror M1 is mounted on a piezo-electric transducer for phase scan and a micrometer for large range location scan. The coincidence window is measured to be 10ns. Under this condition ( $T_R = 10 \text{ ns} \gg \tau$ ), The coincidence rate is given by Eq.(6). The first term of Eq.(6) is a phase dependent term that is always there. In order to concentrate on the second term in Eq.(6) for unbalanced HOM interference effect, we dither the phase

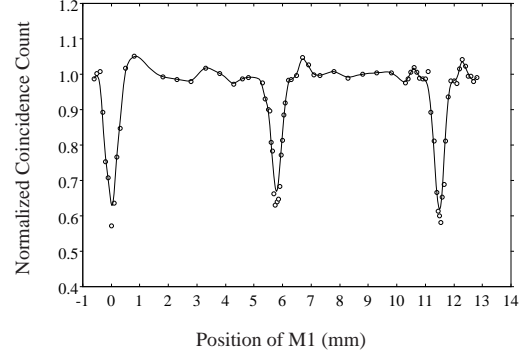


FIG. 4. Normalized coincidence as a function of the micrometer position of mirror M1. The solid line is a smooth interpolation of the data for visual guidance.

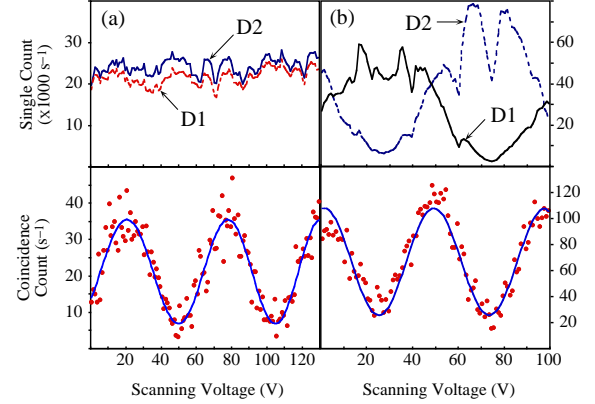


FIG. 5. Coincidence as well as single counts as a function of the voltage of piezoelectric transducer. Micrometer for M1 is set at (a) 5.7 mm and (b) 11.5 mm.

(piezoelectric transducer) so that the contribution from the first term is merely a constant baseline that will limit the HOM interference visibility to a maximum of 50%. In Fig.4, we plot the corrected coincidence counts as a function of the position of M1 (micrometer). The reappearance of the HOM dip at nonzero delays in Fig.4 implies a two-photon correlation function as in Eq.(2) [14]. The data was collected in separate experiments because the interferometer needs to be realigned after some large displacement of M1 (the visibility of the interferometer, which is independently monitored by an auxiliary laser, drops significantly after about 6 mm displacement of M1). So the coincidence data has to be normalized to an average of the points at the wings of the dips. The spacing between dips is 5.75 mm corresponding to one half cavity round trip distance of the OPO cavity.

Next we fix the micrometer position of M1 at the bottom of the two dips with nonzero path differences which correspond to one half and one full cavity round trip distance, respectively. We then scan the phase via the piezoelectric transducer. Fig.5 shows the coincidence as well as the single detector counts as a function of electric voltage at the two micrometer positions of M1. Coincidence

counts at both positions show the sinusoidal interference pattern with visibilities larger than 50%. The solid curves is a least square fit to a SINE function with 68% and 62% visibility, respectively. The low visibility is attributed to poor mode match at large path delays. A surprise from Fig.5b shows that the single detector counts also vary sinusoidally with the phase change and the counts from the two detectors are 180 degree out of phase (The unexpected drops in single counts are due to instability of the OPO cavity and are corrected in coincidence counts). So the interference pattern in coincidence is simply from the anti-correlation of single counts. This is not fourth-order but second-order interference. The reappearance of second-order coherence at nonzero delay can be easily understood by calculating the second-order field correlation function:

$$\begin{aligned} \langle I_1 I_2 \rangle &= \langle \hat{E}^{(+)}(t) \hat{E}^{(+)}(t) \hat{E}^{(+)}(t) \hat{E}^{(+)}(t) \rangle \\ &= e^{i\Delta\omega t} G(\tau) F(\tau) \end{aligned} \quad (7)$$

with  $G(\tau) = \int d\omega \int d\omega' \hat{f}(\omega) \hat{f}(\omega')$ .  $\hat{f}(\omega)$  gives the visibility of interference patterns in single detector counts and it has similar comb-like shape as  $\langle I_1 \rangle$ . So the single count interference pattern revives at various multiples of  $\tau_c$ , just like a mode locked laser. In contrast, interference pattern in coincidence occurs with a period of  $\tau_c=2$ . For those micrometer positions of  $M_1$  that are not inside any of the dips in Fig.4, no interference arises from the second term of Eq.(6). This term simply adds a constant to the baseline to reduce the visibility to maximum of 50%. This corresponds to the simple scheme of Franson interferometer [12]. We observed a visibility of around 35% at those locations.

The interesting comb-like correlation function can be used for quantum state engineering. Here we propose to use two-photon interference to take out one of the spikes in the correlation function (Fig.1). To do that, we consider a wide band two-photon state described by

$$\begin{aligned} | \Psi \rangle &= \int d\omega \int d\omega' \hat{E}^{(+)}(\omega) \hat{E}^{(+)}(\omega') | \text{vac} \rangle \\ &= \int d\omega \int d\omega' \hat{E}^{(+)}(\omega) \hat{E}^{(+)}(\omega') | \text{vac} \rangle; \end{aligned} \quad (8)$$

where  $\hat{E}^{(+)}(\omega)$  gives the wide spectrum of down-conversion and  $\tau$  sets a relative delay between the two photons. The two-photon correlation function is simply

$$\langle I_1 I_2 \rangle = \langle \hat{E}^{(+)}(\omega) \hat{E}^{(+)}(\omega') \hat{E}^{(+)}(\omega) \hat{E}^{(+)}(\omega') \rangle$$

This is a single peaked function centered at  $\tau=0$ .

We mix this state with the mode-locked two-photon state in Eq.(1). The actual state of the system is

$$| \Psi \rangle = (| \text{vac} \rangle + | \Psi_L \rangle) (| \text{vac} \rangle + | \Psi_B \rangle); \quad (9)$$

Here we add in the vacuum state to write the true states from parametric down-conversion and the coefficients and are related to a common pump field. We can easily

calculate the time correlation function of the combined field as

$$\langle I_1 I_2 \rangle = \langle \hat{E}^{(+)}(\omega) \hat{E}^{(+)}(\omega') \hat{E}^{(+)}(\omega) \hat{E}^{(+)}(\omega') \rangle \quad (10)$$

If  $\hat{E}^{(+)}(\omega)$  overlaps with one of the peaks of  $\hat{E}^{(+)}(\omega')$ , destructive interference will take out that peak with proper adjustment of  $\omega$  and  $\omega'$ . By changing the delay  $\tau$ , we can manage to take any one out for information coding.

In conclusion, we have applied the concept of mode locking to entangled two-photon state and observed its effects in an unbalanced HOM interferometer. Quantum interference can be used to manipulate the entanglement in time domain.

#### ACKNOWLEDGMENTS

We'd like to thank P. Kumar for pointing us to Ref. [14] and suggesting a possible experiment. This work was supported by Purdue Research Foundation and NSF.

- 
- [1] Y. H. Shih and C. O. Alley, Phys. Rev. Lett. 61, 2921 (1988); Z. Y. Ou and L. Mandel, Phys. Rev. Lett. 61, 50 (1988).
  - [2] P. Grangier, M. J. Patasek, and B. Yurke, Phys. Rev. A 38, 3132 (1988).
  - [3] Z. Y. Ou and L. Mandel, Phys. Rev. Lett. 61, 54 (1988).
  - [4] H. H. A. Maat and G. A. Barbosa, Phys. Rev. Lett. 85, 286 (2000); A. Mair et al, Nature 412, 313 (2001).
  - [5] K. Mattle et al, Phys. Rev. Lett. 76, 4656 (1996).
  - [6] D. Bouwmeester et al, Nature 390, 575 (1997).
  - [7] S. P. Walborn et al, Phys. Rev. Lett. 90, 143601 (2003).
  - [8] M. Bellini et al, Phys. Rev. Lett. 90, 043602 (2003).
  - [9] X. Y. Zou et al, Phys. Rev. Lett. 69, 3041 (1992).
  - [10] See, for example, A. E. Siegman, Lasers, University Science Books, (Mill Valley, CA, 1986).
  - [11] C. K. Hong, Z. Y. Ou, L. Mandel, Phys. Rev. Lett. 59, 2044 (1987).
  - [12] J. D. Franson, Phys. Rev. Lett. 62, 2205 (1989).
  - [13] Z. Y. Ou et al, Phys. Rev. Lett. 65, 321 (1990); P. G. Kwiat et al, Phys. Rev. A 41, 2910 (1990).
  - [14] J. H. Shapiro, Technical Digest of Topical Conference on Nonlinear Optics, p.440, FC7-1, Optical Society of America (2002).
  - [15] T. B. Pittman et al, Phys. Rev. Lett. 77, 1917 (1996).
  - [16] Z. Y. Ou and Y. J. Lu, Phys. Rev. Lett. 61, 2557 (1999); Y. J. Lu and Z. Y. Ou, Phys. Rev. A 62, 033804 (2000).